Development 140, 2149-2159 (2013) doi:10.1242/dev.090688

HECT-E3 ligase ETC-1 regulates securin and cyclin B1 cytoplasmic abundance to promote timely anaphase during meiosis in *C. elegans*

Ruishan Wang[1,*,‡], Zeenia Kaul[2,*,§], Charuta Ambardekar[2], Takaharu G. Yamamoto[1,¶], Kanisha Kavdia[3], Kiran Kodali[3], Anthony A. High[3] and Risa Kitagawa[2,#]

SUMMARY

The anaphase inhibitor securin plays a crucial role in regulating the timing of sister chromatid separation during mitosis. When sister chromatid pairs become bioriented, the E3 ligase anaphase promoting complex/cyclosome (APC/C) ubiquitylates securin for proteolysis, triggering sister chromatid separation. Securin is also implicated in regulating meiotic progression. Securin protein levels change sharply during cell cycle progression, enabling its timely action. To understand the mechanism underlying the tightly regulated dynamics of securin, we analyzed the subcellular localization of the securin IFY-1 during *C. elegans* development. IFY-1 was highly expressed in the cytoplasm of germ cells. The cytoplasmic level of IFY-1 declined immediately following meiosis I division and remained low during meiosis II and following mitoses. We identified a *C. elegans* homolog of another type of E3 ligase, UBE3C, designated ETC-1, as a regulator of the cytoplasmic IFY-1 level. RNAi-mediated depletion of ETC-1 stabilized IFY-1 and CYB-1 (cyclin B1) in post-meiosis I embryos. ETC-1 knockdown in a reduced APC function background caused an embryonic lethal phenotype. *In vitro*, ETC-1 ubiquitylates IFY-1 and CYB-1 in the presence of the E2 enzyme UBC-18, which functions in pharyngeal development. Genetic analysis revealed that UBC-18 plays a distinct role together with ETC-1 in regulating the cytoplasmic level of IFY-1 during meiosis. Our study reports a novel mechanism, mediated by ETC-1, that co-operates with APC/C to maintain the meiotic arrest required for proper cell cycle timing during reproduction.

KEY WORDS: Securin, *Caenorhabditis elegans*, Anaphase promoting complex, HECT-E3 ligase

INTRODUCTION

The anaphase inhibitor securin plays a key role as a mitotic substrate of the anaphase promoting complex/cyclosome (APC/C) by regulating the timing of sister chromatid separation (Musacchio and Salmon, 2007). It binds and inhibits separase, a protease that cleaves the cohesin component Scc1/Rad21. Once all pairs of sister chromatids have achieved bipolar spindle attachment via the kinetochore, APC/C targets securin for ubiquitin-mediated proteolysis. This degradation of securin allows separase to cleave Scc1/Rad21, leading to sister chromatid separation.

In budding yeast, the recognition and ubiquitylation of securin by APC/C is regulated by the phosphorylation status of securin, which is controlled by Cdk1 and Cdc14 (Holt et al., 2008). As budding yeast Cdc14 is activated by separase (Stegmeier et al., 2002; Queralt et al., 2006), this Cdk1-Cdc14-mediated regulation of securin stability is likely to constitute a positive-feedback loop that leads to sudden and rapid destruction of securin to enable the switch-like activation of separase. Chromosome missegregation frequency is high in unphosphorylatable securin mutants (Holt et al., 2008), suggesting that abrupt destruction of securin is crucial to maintain chromosome stability. In mouse oocytes, accumulation of securin titrates APC/C activity, thereby increasing the stability of another mitotic APC/C substrate, cyclin B1, to drive entry into M phase (Marangos and Carroll, 2008).

The APC/C-mediated regulatory system also controls meiotic progression (Pesin and Orr-Weaver, 2008). During meiosis, two rounds of chromosome segregation occur sequentially, without an intervening S phase, to generate haploid cells. During meiotic prophase, each pair of homologous chromosomes is connected via the meiotic cohesin complex, in which the mitotic cohesin component Scc1/Rad21 is replaced by the meiosis-specific cohesin component Rec8 (Parisi et al., 1999; Lee et al., 2003; Xu et al., 2005). Meiotic cohesin also connects sister chromatid pairs until meiosis II division. Separase cleaves Rec8 for onset of anaphase I and anaphase II.

The requirement for APC/C-mediated degradation of securin to activate separase for Rec8 removal from meiotic chromosomes is a widely conserved mechanism in the reproduction process in eukaryotes. In *C. elegans*, mutational inactivation or RNAi-mediated knockdown of APC/C components causes meiotic metaphase I arrest (Furuta et al., 2000; Golden et al., 2000; Davis et al., 2002; Shakes et al., 2003; Shakes et al., 2011). Similarly, knockdown of APC/C activators FZY-1/Cdc20, IFY-1/securin and SEP-1/separase causes metaphase I arrest (Siomos et al., 2001; Kitagawa et al., 2002; Shakes et al., 2003). The temperature-sensitive allele of APC/C components exhibits abnormalities in both

[1]Department of Molecular Pharmacology, St Jude Children's Research Hospital, Memphis, TN 38105, USA. [2]Center for Childhood Cancer, The Research Institute at Nationwide Children's Hospital, Columbus, OH 43205, USA. [3]Proteomics Core, St Jude Children's Research Hospital, Memphis, TN 38105, USA.

*These authors contributed equally to this work
‡Present address: Department of Pharmacology, University of Tennessee Health Science Center, Memphis, TN 38163, USA
§Present address: Department of Molecular Virology, Immunology and Medical Genetics, The Ohio State University Wexner Cancer Center, College of Medicine, Columbus, OH 43210, USA
¶Present address: Cell Biology Group, Advanced ICT Research Institute, National Institute of Information and Communications Technology, Kobe 651-2492, Japan
#Author for correspondence (risa.kitagawa@nationwidechildrens.org)

Accepted 9 March 2013

meiosis I and II at semi-permissive temperature. However, defects during meiosis II include a failure in sister chromatid separation and meiosis II spindle elongation but not metaphase II arrest; therefore, whether APC/C activity is required for the onset of anaphase II remains unclear.

In *C. elegans*, in addition to APC/C, another type of E3 ligase, cullin 2 (CUL-2), plays a crucial role in meiotic progression (Liu et al., 2004; Sonneville and Gönczy, 2004; Vasudevan et al., 2007). Loss of function of the elongin–CUL-2–RBX-1 E3 ligase complex or its substrate-specific adaptor, ZYG-11, delays the onset of anaphase II and exit from meiosis II (Liu et al., 2004; Sonneville and Gönczy, 2004; Vasudevan et al., 2007). Depletion of CUL-2 or ZYG-11 causes accumulation of cyclins B1 and B3, but it remains unclear whether these cyclins are the targets of CUL-2 and ZYG-11 or accumulate as an indirect consequence of the accumulation of other CUL-2 targets. For faithful chromosome transmission during meiosis and mitosis, other ubiquitin E3 ligases might function synergistically or independently to achieve the ubiquitin-mediated proteolysis essential for proper cell cycle progression. To understand the molecular mechanism underlying the coordination of cell cycle events, it is important to identify the E3 ligase and its substrate for proteolysis.

We have previously reported that IFY-1 acts as securin in *C. elegans* embryos (Kitagawa et al., 2002). IFY-1 interacts with the APC/C activator FZY-1 and separase SEP-1. IFY-1 accumulates in APC/C-defective embryos. Also, RNAi-mediated depletion of IFY-1 phenocopies SEP-1-defective embryos. Unlike Pds1 in budding yeast and Pttg1 in mouse [which act as securin to maintain chromosome stability but are dispensable for growth and fertility (Yamamoto et al., 1996; Jallepalli et al., 2001)], IFY-1 has an essential function during meiotic progression and IFY-1-depleted embryos arrest before anaphase I (Kitagawa et al., 2002).

Here, we show that ETC-1, a HECT-E3 ligase, regulates the stability of cytoplasmic IFY-1 and CYB-1 in post-meiosis I *C. elegans* embryos. An *in vitro* ubiquitylation assay revealed that ETC-1 ubiquitylates IFY-1 and CYB-1 in the presence of the E2 enzyme UBC-18. These data and those obtained from RNAi-mediated functional analysis suggest that ETC-1 and UBC-18 target cytoplasmic IFY-1 and CYB-1 for ubiquitin-mediated proteolysis independently of APC/C, thereby leading to rapid degradation of cytoplasmic IFY-1 and CYB-1 after anaphase I.

MATERIALS AND METHODS

Strains and alleles

C. elegans strains and alleles are listed in supplementary material Table S1. Transgenic worms were generated by ballistic transformation with expression vectors using PDS-1000 (Bio-Rad) as described (Praitis et al., 2001).

RNAi

RNAi was performed by feeding with double-stranded RNA (dsRNA)-expressing bacteria or by the soaking method, as described previously (Maeda et al., 2001; Kamath and Ahringer, 2003). RNAi vectors for targeting *apc-2*, *sep-1*, *ubc-18*, *ify-1* and *etc-1* were retrieved from the Ahringer *C. elegans* RNAi feeding library (Wellcome/CRC Institute, University of Cambridge, UK) (Kamath and Ahringer, 2003) obtained from Geneservice (Cambridge, UK). The L4440 RNAi vector (pPD129.36) was used as an RNAi empty vector control. For *etc-1* RNAi, bacterial cells in induced culture were pelleted and resuspended in M9 buffer. Aliquots were frozen and stored at –80°C. For each experiment, the bacterial suspension was freshly thawed and seeded onto nematode growth medium (NGM) plates. Worms were transferred to newly seeded plates every 24 hours for 4 days. For co-depletion of IFY-1 and ETC-1, equal volumes of *ify-1*(RNAi) and *etc-1*(RNAi) bacterial cell suspensions were thoroughly mixed and plated. For depletion of IFY-1 alone as a control, the *ify-1*(RNAi) bacterial cell suspension was mixed with an equal volume of *Escherichia coli* OP50 cell suspension.

RT-PCR

For RT-PCR analysis of *etc-1* expression, total RNA was extracted using Trizol according to the manufacturer's protocol (Invitrogen, Carlsbad, CA, USA). DNA contamination was removed by incubation with DNase I at 37℃ for 20 minutes. One-step RT-PCR was performed using QIAGEN OneStep PT-PCR kit according to the manufacturer's protocol (Qiagen) with primers (5′-3′): *etc-1*, CTGAGTGGAATCGGAGAACA and GAGGTCGGCTTGATATGATCT; *actin* (internal control), CGGTATGGGACAGAAGGACT and GTGCTCGATTGGGTACTTCA.

Microscopy

For time-lapse movies of embryos *in utero*, young adult hermaphrodites were anesthetized with 0.0125% tetramisole (Sigma) in M9 and mounted on 1% agarose pads with a thin layer of mineral oil between the coverslip and pad. A set of images at three focal planes at 2 μm intervals was taken at each time point. Live images were taken by a DM IRE2 motorized fluorescence microscope (Leica Microsystems, Allendale, NJ, USA) equipped with a Plan Apo 63× lens (NA=1.4, Leica) and an ORCA-ER high-resolution digital CCD camera (Hamamatsu, Bridgewater, NJ, USA) under the control of Openlab software (Improvision, Lexington, MA, USA). IFY-1-GFP and GFP-CYB-1 levels were quantitated by measuring the fluorescent signal with Openlab and subtracting background fluorescence. When collecting data from each embryo, the intensity of the signal in an oocyte at the −1 position was also measured and used to calculate the value for each embryo relative to the −1 oocyte. For still images, 10-15 focal planes at 1 μm intervals were taken and processed into extended-focus images using Volocity software (Improvision).

Immunofluorescence experiments were performed as described (Watanabe et al., 2008). The primary antibody for immunofluorescence microscopy was anti-REC-8 (Pasierbek et al., 2001). The secondary antibody was Alexa Fluor 594-conjugated anti-rabbit IgG antibody (Molecular Probes). To visualize DNA, 1 μg/ml DAPI was added to the secondary antibody solution.

Antibody preparation

The N-terminal half of *etc-1* cDNA (bp 1-1416) was cloned into pGEX4T1 (GE Healthcare, Piscataway, NJ, USA). Bacterially expressed and purified GST-ETC-1Nter (amino acids 1-472) was used to immunize two rabbits. Antisera were generated by Pocono Rabbit Farm and Laboratory (PRF&L, Canadensis, PA, USA). Immune sera were depleted of anti-GST antibodies by passages through a GST-coupled column; then, anti-ETC-1 antibody was purified on GST-ETC-1 immobilized on a PVDF membrane and eluted with 100 mM glycine (pH 2.5). Eluate was neutralized with 2 M Tris-HCl (pH 8.5) and dialyzed against PBS (pH 7.4) containing 10% glycerol.

Immunoprecipitation and mass spectrometry

The protein lysate was prepared from gravid worms expressing GFP and IFY-1-GFP (strains RQ281 and RQ423, respectively) grown at 16°C, and immunoprecipitation was performed with anti-GFP antibody as described (Watanabe et al., 2008). Immunoprecipitates were separated on 4-12% Nu-PAGE (Invitrogen) and stained with SYPRO Ruby (Invitrogen). Gel slices containing protein bands in IFY-1-GFP immunoprecipitates and those at corresponding positions in immunoprecipitates with GFP alone were excised, reduced, and alkylated with iodoacetamide and digested with trypsin. Tryptic peptides were analyzed by liquid chromatography with tandem mass spectrometry (LC-MS/MS) at the Proteomics Core Facility (St Jude Children's Research Hospital, Memphis, TN, USA) using an LTQ linear ion trap mass spectrometer (ThermoElectron, San Jose, CA, USA). Database searches were performed using LTQ.raw files in combination with the Mascot search engine (Matrix Science). The proteins identified are described in supplementary material Table S2.

For the co-immunoprecipitation assay, GFP, IFY-1-GFP and GFP-CYB-1 were immunoprecipitated with anti-GFP antibody or rabbit IgG from the whole-worm protein lysate prepared from strains RQ281, RQ386, RQ414, and N2. Immunoprecipitates were separated on 4-12% Nu-PAGE and

transferred to a PVDF membrane. The membrane was divided in two at the position of the 102 kDa marker protein. The top portion (proteins larger than 102 kDa) was blotted with anti-ETC-1 antibody. The bottom portion (proteins smaller than 102 kDa) was blotted with anti-GFP mouse monoclonal antibody (Roche Diagnostics, Indianapolis, IN, USA).

In vitro ubiquitylation assay

The His6-IFY-1 expression vector was constructed by cloning a full-length *ify-1* cDNA into pRSETA (Invitrogen). To construct the CYB-1-His6 expression vector, full-length *cyb-1* cDNA was amplified by PCR from a yeast two-hybrid cDNA (RB1) library (gift from Robert Barstead, University of Oklahoma Health Sciences Center, Oklahoma City, OK, USA) using specific primers (a T7 promoter sequence and a His-6 coding sequence were added to the forward and reverse primers, respectively) and cloned into a pBluescript SKII plasmid (Stratagene, La Jolla, CA, USA). The His6-EGFP expression vector pET9d-EGFP was described previously (Meacci et al., 2006) and kindly provided by Karsten Kruse (Max-Planck Institute for the Physics of Complex Systems, Dresden, Germany). GST-ETC-1 expression vector was constructed by cloning a full-length cDNA of *etc-1* into pGEX4T1. Expression vectors for GST-WWP-1 and GST-UBC-18 were obtained from Andrea Carrano and Andrew Dillin (The Salk Institute for Biological Studies, La Jolla, CA, USA), and for GST-APC-11, GST-APC-11m and His6-UBC-2 were obtained from Lynn Boyd (University of Alabama in Huntsville, Huntsville, AL, USA). GST-APC-11m is GST fused mutant APC-11, in which a cysteine in position 100 of the RING finger of APC-11 was replaced with a leucine, and used as an E3 ligase inactive control for the in vitro ubiquitylation assay (Frazier et al., 2004).

To express fusion proteins for use in ubiquitylation assays, 30 ml of a saturated culture of BL21 bacteria carrying individual expression plasmids was inoculated into 1 liter of LB medium containing 100 μg/ml ampicillin and grown to an optical density of 0.3-0.5 at 37°C. Cultures were induced for 2-4 hours by adding IPTG to a final concentration of 1 mM. His6-IFY-1, CYB-1-His6, His6-EGFP and His6-UBC-2 were purified under nondenaturing conditions using nickel-nitrilotriacetic acid (Qiagen, Germantown, MD, USA). GST, GST-ETC-1, GST-WWP-1, GST-APC-11 and GST-APC-11m were purified by glutathione S-transferase (GST) chromatography (GE Healthcare, Waukesha, WI, USA). The GST tag on UBC-18 was removed by thrombin cleavage, and thrombin was absorbed by incubating with benzamidine Sepharose 4B beads. Eluted proteins were dialyzed against ubiquitylation buffer (50 mM Tris pH 8.0, 5 mM $MgCl_2$, 2 mM NaF, 0.5 mM DTT) or storage buffer (50 mM HEPES pH 8.0, 100 mM NaCl, 10% glycerol). To check the purity and the amount of GST-proteins used for the assay, purified samples were separated on SDS-PAGE, and visualized by staining the gel with Simply Blue. His6-proteins were separated on SDS-PAGE, transferred to a PVDF membrane, then blotted with anti-penta his antibody.

Ubiquitylation assays were performed in a reaction volume of 30 μl in ubiquitylation buffer for 1.5 hours at 32°C. The reaction mixture consisted of 550 ng/μl UBE1 (Boston Biochem, Cambridge, MA, USA), 1.8 μg/μl UBC-2 or UBC-18, 20-25 μg GST-fused E3 ubiquitin ligases, 100 mM ATP and 10 μg/μl hemagglutinin-tagged ubiquitin (HA-Ub). Sample buffer was added to stop the reaction. The reaction mixture was separated on SDS-PAGE and transferred to a PVDF membrane. Ubiquitylation and substrate modification were detected by probing with anti-HA antibody (rat monoclonal, 1:1000; Roche) and anti-His antibody (mouse monoclonal, 1:2000; Qiagen), respectively. The detection was performed with chemiluminescent reagents (GE Healthcare).

RESULTS

Dynamic change in the subcellular localization of IFY-1 during meiosis and mitosis

To further characterize the physiological function of IFY-1, we generated a transgenic worm strain expressing IFY-1 fused at the C-terminus with GFP (IFY-1-GFP) under the control of its endogenous promoter and 3′ region (supplementary material Fig. S1). The *ify-1* mutant allele *tm947* contains a genomic deletion of 648 bp, from –594 bp to +53 bp of the *ify-1* coding sequence, and is therefore likely to be a null allele. *tm947* homozygotes derived from heterozygous parents exhibited an embryonic lethal phenotype (supplementary material Table S1). IFY-1-GFP expression suppressed the embryonic lethality of *tm947* homozygotes, suggesting that IFY-1-GFP is functional. Although *tm947* also deletes *rpl-22* from –520 bp to +127 bp, which encodes an essential ribosomal protein large subunit on the complementary strand, our construct also contains the entire *rpl-22* coding region and an adequate level of RPL-22 is likely to be expressed from the transgene. The spatiotemporal dynamics of IFY-1 expression was determined throughout development using a strain expressing IFY-1-GFP in an *ify-1* null background (*tm947* homozygotes).

Fluorescence microscopy analysis identified substantial levels of IFY-1-GFP in the cytoplasm of germ cells (Fig. 1A). The cytoplasmic IFY-1-GFP was maintained at a high level during oocyte maturation. Upon nuclear envelope breakdown (NEBD) in mature oocytes, IFY-1-GFP began associating with chromosomes and meiosis I spindle microtubules, and remained associated with them during meiosis I but disappeared immediately after homologous chromosome separation (anaphase I) (Fig. 1B). Cytoplasmic levels of IFY-1-GFP were also reduced immediately after chromosomal IFY-1-GFP degradation and maintained at a low level during meiosis II and the following mitoses. This drastic change in the total cellular level of IFY-1 during meiosis is comparable to securin dynamics in mouse oocytes (Nabti et al., 2008; McGuinness et al., 2009).

There was no appreciable chromosomal association of IFY-1-GFP fluorescence signal in embryonic cells undergoing mitosis during early stage embryogenesis (supplementary material Fig. S2A). However, when a spindle checkpoint-dependent mitotic delay was induced by CYB-3 depletion (Deyter et al., 2010), chromosome-associated IFY-1 was seen (supplementary material Fig. S2A), suggesting that IFY-1 is stabilized as a result of inhibition of APC/C by the spindle checkpoint. Also, there was cell cycle-dependent chromosomal association of IFY-1 in embryos developing further than the 4E stage (50-90 cells) (supplementary material Fig. S2B). The cell cycle lengths of blastomeres during 4E are longer than during the early stage (Bao et al., 2008). Given that the IFY-1-GFP signal became detectable even during early stage embryogenesis if the cell cycle length was extended by CYB-3 depletion, it is possible that IFY-1-GFP needs to be newly synthesized before mitosis in each round of the cell cycle and becomes detectable only when the cell cycle length is long enough for it to become fluorescent (by being properly folded). Alternatively, control of the chromosomal association of IFY-1 during the early and later stages of embryogenesis might be distinct. Taken together, the association of IFY-1 with mitotic chromosomes in a cell cycle-dependent manner suggests its role as a securin during mitosis.

A HECT-E3 ligase regulates IFY-1 dynamics

C. elegans proteins were screened by immunoprecipitation-mass spectrometry analysis to identify those that associate with IFY-1. Forty-seven proteins were identified in IFY-1-GFP co-immunoprecipitates, including 31 proteins also identified in co-immunoprecipitates with GFP alone (supplementary material Fig. S3). SEP-1, a known IFY-1 interactor, was one of the 16 proteins identified specifically in IFY-1-GFP co-immunoprecipitates (supplementary material Table S2).

To determine which of these candidate IFY-1-associated proteins are required for proper function of IFY-1, we analyzed the effect of

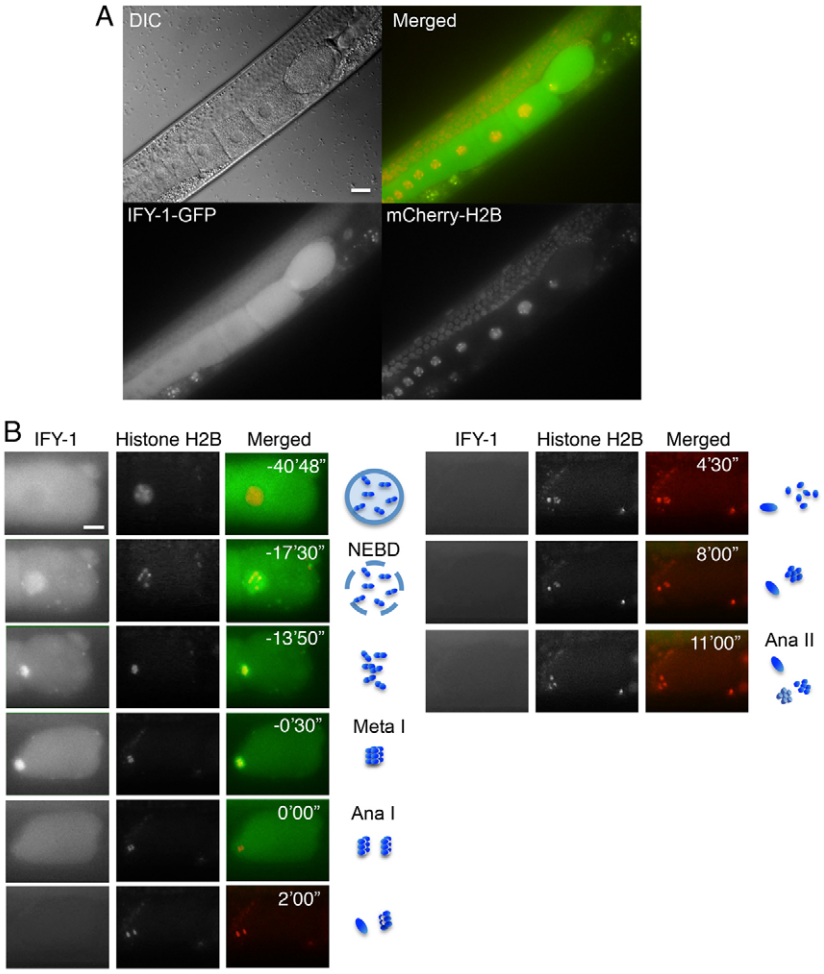

Fig. 1. Expression of IFY-1-GFP in *C. elegans* germ cells. (**A**) Differential interference contrast (DIC) and fluorescence microscopy images of a gonad arm of an adult hermaphrodite expressing IFY-1-GFP (green) and mCherry-histone H2B (red). The IFY-1-GFP signal was identified in the cytoplasm of germ cells in premeiotic stages, prophase I and meiosis I. (**B**) IFY-1-GFP dynamics during meiotic division. Time-lapse microscopy images of a mature oocyte expressing IFY-1-GFP and mCherry-histone H2B. Time (minutes, seconds) relative to the onset of anaphase is shown on the merged images. Nuclear morphology and the phases of the meiotic stage are illustrated on the right. NEBD, nuclear envelope breakdown; Meta I, metaphase I; Ana I, anaphase I; Ana II, anaphase II. Scale bars: 10 μm.

their RNAi knockdown on the subcellular dynamics of IFY-1-GFP. First, we confirmed whether IFY-1 dynamics is affected by reduction of APC/C activity or depletion of its binding partner SEP-1. Depletion of an APC/C component (e.g. APC-2) or a substrate-specific activator of APC/C (e.g. FZY-1) causes strict arrest of meiotic embryos before anaphase I (Golden et al., 2000; Kitagawa et al., 2002). In these arrested embryos, IFY-1-GFP remained associated with meiotic chromosomes and the cytoplasmic level of IFY-1-GFP remained high (Fig. 2A). SEP-1-depleted embryos were also arrested in meiosis I and failed to progress to meiosis II. In SEP-1-depleted oocytes, IFY-1-GFP entered the nuclei before NEBD (supplementary material Fig. S4). During meiosis I, there was no detectable association of IFY-1-GFP with chromosomes (Fig. 2A; supplementary material Fig. S4). These observations suggest that IFY-1 is retained in the cytoplasm when it forms a complex with SEP-1 during interphase, and the IFY-1–SEP-1 complex is recruited to meiotic chromosomes after NEBD in an SEP-1-dependent manner. In SEP-1-depleted embryos, an IFY-1-GFP signal coincident with the meiosis I spindle was still detectable (Fig. 2A; supplementary material Fig. S4), suggesting that IFY-1 associates with the meiosis I spindle independently of SEP-1. The budding yeast securin Pds1 also localizes to the spindle independently of the separase Esp1 (Jensen et al., 2001), suggesting that IFY-1 possesses a conserved securin function.

We identified the D2085.4 gene product with eight unique tryptic peptides, which cover 11.6% of the entire protein (supplementary material Table S2), as an IFY-1 interactor. The D2085.4 gene product has sequence similarity with the human HECT domain-containing E3 ligase UBE3C (supplementary material Fig. S5); therefore, we refer to this protein as ETC-1 [from UB*E* *T*hree *C-1*]. Our RNAi screen revealed that knockdown of ETC-1 altered IFY-1 stability during meiotic division. We performed RNAi-mediated ETC-1 knockdown by feeding worms with *etc-1* dsRNA-expressing bacteria, which reduced the endogenous *etc-1* mRNA level to less than 10% of that in untreated worms (supplementary material Fig. S6A). The effectiveness of *etc-1* RNAi by the feeding method was also confirmed by substantial reduction of the GFP signal in transgenic embryos expressing GFP-ETC-1 (supplementary material Fig. S6B).

The expression pattern of IFY-1-GFP in *etc-1*(RNAi) germ cells was comparable to that in untreated controls until germ cells entered meiosis II (supplementary material Fig. S7). The stability of cytoplasmic IFY-1-GFP during meiosis II appeared altered in *etc-1*(RNAi) embryos (Fig. 2A,B; supplementary material Fig. S7). In untreated embryos, the cytoplasmic IFY-1-GFP signal drastically diminished immediately after the disappearance of chromosome-associated IFY-1-GFP. However, in *etc-1*(RNAi) embryos the cytoplasmic IFY-1-GFP signal gradually reduced after anaphase I, but ~50% of the signal remained in the cytoplasm during meiosis II (Fig. 2A,B). Thus, RNAi knockdown of ETC-1 substantially stabilized cytoplasmic IFY-1 in post-meiosis I embryos.

Corresponding to the stabilization of IFY-1 in post-meiosis I embryos, the duration of meiosis II (the interval between the onset of anaphase I and anaphase II) was substantially extended in *etc-*

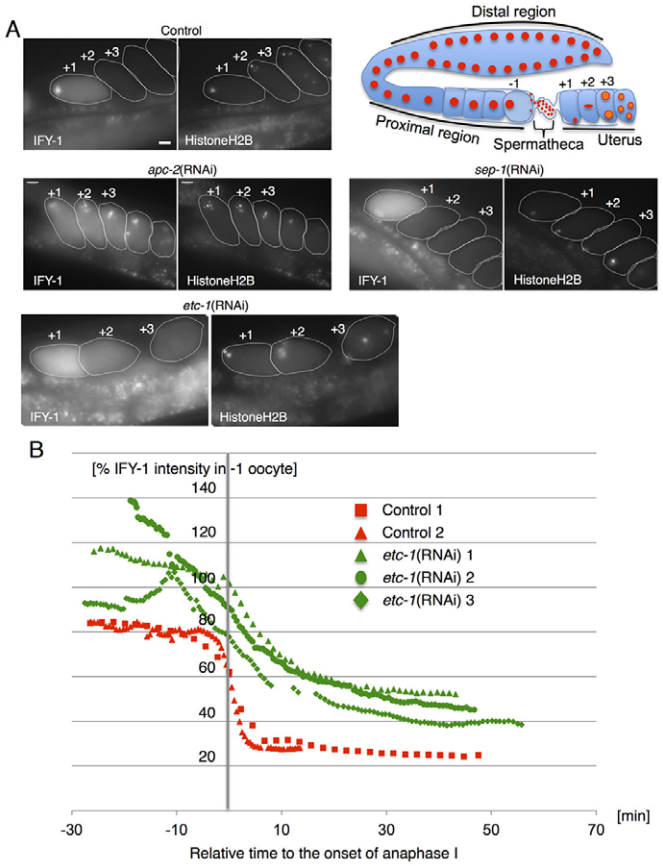

Fig. 2. RNAi-mediated depletion of ETC-1-stabilized IFY-1 in post-meiosis I embryos. (**A**) Fluorescence images of untreated, *apc-2*(RNAi), *sep-1*(RNAi) and *etc-1*(RNAi) embryos expressing IFY-1-GFP and mCherry-histone H2B. Embryos in uterus are outlined and positions are labeled (the position closest to the spermatheca is +1, see schematic of gonad arm). The cytoplasmic IFY-1-GFP signal was immediately reduced after meiosis I in untreated embryos but remained in *apc-2*(RNAi) embryos. In untreated embryos, IFY-1-GFP localized to meiotic chromosomes during meiosis I as well as to the cytoplasm, but was not associated with chromosomes in *sep-1*(RNAi) embryos. In *etc-1*(RNAi) embryos, cytoplasmic IFY-1-GFP was maintained at a higher level than that in untreated embryos. (**B**) Time-lapse analysis of cytoplasmic IFY-1-GFP fluorescence intensity during meiosis. Data were collected under the same conditions for each embryo [two control and three *etc-1*(RNAi) embryos are shown] and are presented relative to the intensity in an embryo at position –1 (the most proximal end of a gonad). Scale bar: 10 μm.

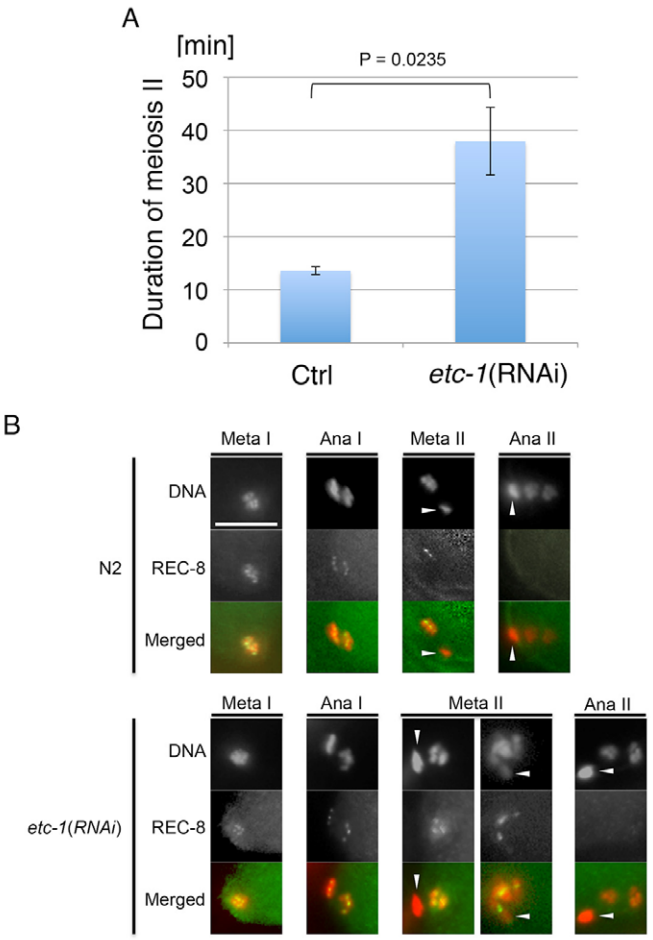

Fig. 3. RNAi-mediated depletion of ETC-1 extends the duration of meiosis II and causes retention of REC-8 at sister chromatid cohesion. (**A**) The duration of meiosis II, defined as the interval between anaphase I and anaphase II, was measured in untreated (Ctrl) or *etc-1*(RNAi) embryos and the average of data from more than three embryos was plotted. The *P*-value versus untreated control is shown. Error bars indicate s.d. (**B**) Untreated (N2) or *etc-1*(RNAi) embryos at the indicated meiotic stages were fixed and stained with DAPI and anti-REC-8 antibody (pseudocolored red and green in merged images, respectively). The first polar bodies are indicated by arrowheads. In *etc-1*(RNAi) embryos, REC-8 was retained between sister chromatids during extended meiosis II. Scale bar: 10 μm.

1(RNAi) embryos (Fig. 3A). Since anaphase II is triggered by cleavage of the meiosis-specific cohesin subunit REC-8 by SEP-1, this extension might be a consequence of SEP-1 inhibition by the stabilized IFY-1. Consistent with this hypothesis, immunostaining analysis revealed that REC-8 remained between sister chromatids during the extended meiosis II in *etc-1*(RNAi) embryos (Fig. 3B).

ETC-1 also regulates CYB-1 stability during meiosis

Deficiency of the cullin family protein CUL-2 causes extended meiosis II (Liu et al., 2004; Sonneville and Gönczy, 2004). The delay in anaphase II of a *cul-2*-defective mutant depends on stabilization of the cyclin B1 CYB-1 (Liu et al., 2004). We analyzed the effect of ETC-1 depletion on the stability of CYB-1, using GFP-CYB-1-expressing embryos. In wild-type embryos, the GFP-CYB-1 signal accumulated in mature oocytes and immediately diminished as meiotic division progressed (Fig. 4A). In *etc-1*(RNAi) embryos there was a high level of GFP-CYB-1 in the cytoplasm of meiotic embryos and postmeiotic cells (Fig. 4A). Thus, ETC-1 is required to regulate the cytoplasmic level of not only IFY-1 but also CYB-1.

Upon onset of anaphase I, APC/C targets securin and cyclin B1 for ubiquitin-mediated proteolysis. Upregulated securin competes with cyclin B for APC/C-mediated degradation, thereby regulating entry into M phase in mouse oocytes (Marangos and Carroll, 2008). Therefore, ETC-1 knockdown might indirectly stabilize CYB-1 by causing accumulation of IFY-1, which would compete with CYB-1 for APC/C-mediated degradation. We tested this possibility by analyzing the effect of co-depleting IFY-1 and ETC-1 on CYB-1 stability. When GFP-CYB-1-expressing gonad was depleted of IFY-

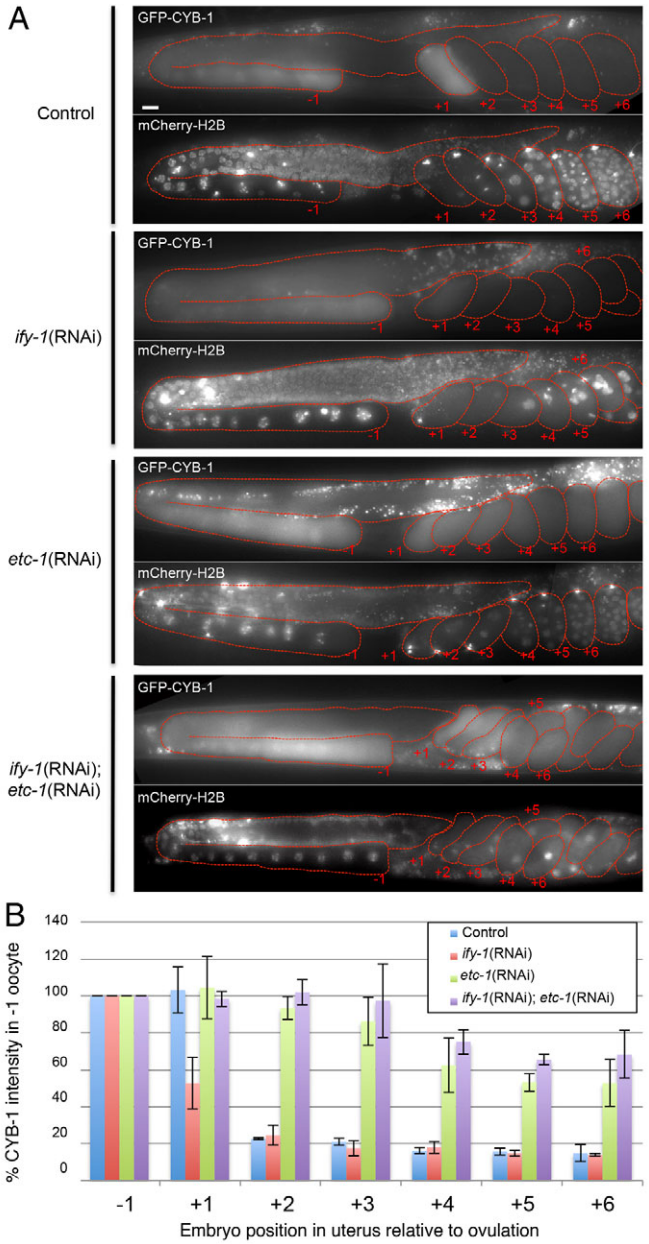

Fig. 4. RNAi-mediated depletion of ETC-1 stabilizes CYB-1 in postmeiotic embryos independently of IFY-1 accumulation. (**A**) Fluorescence microscopy images of embryos expressing GFP-CYB-1 and mCherry-histone H2B after RNAi-mediated knockdown of *ify-1* or *etc-1* or both. A gonad arm and embryos in uterus are outlined. (**B**) Quantitative analysis of cytoplasmic GFP-CYB-1 fluorescence intensity in fertilized embryos. The intensity of GFP-CYB-1 signal in each embryo at the indicated position (the embryo position relative to ovulation) was measured and the value relative to the intensity in an embryo at position –1 (the most proximal end of a gonad) was determined. The average value from three worms is plotted. Error bars indicate s.d. Scale bar: 10 μm.

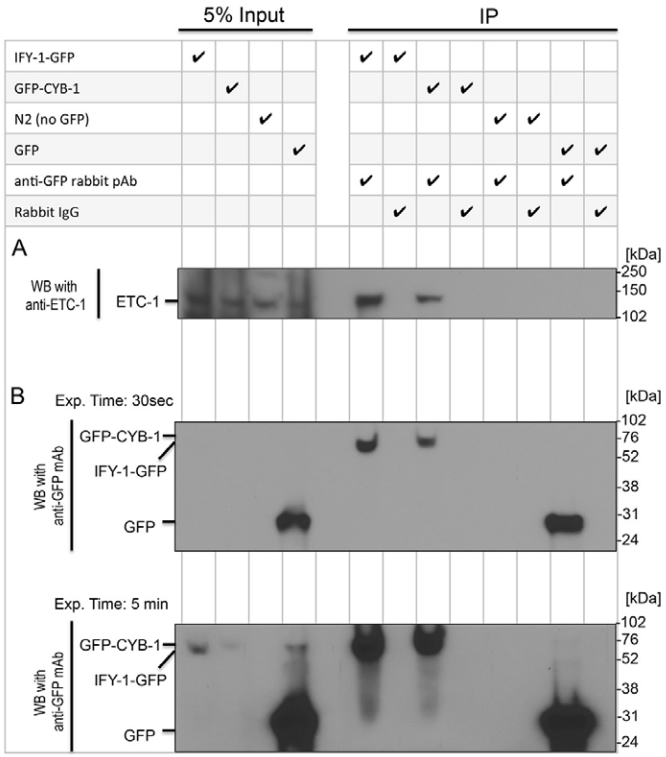

Fig. 5. ETC-1 physically interacts with IFY-1 and CYB-1 *in vivo*. Whole-worm lysates were prepared from gravid hermaphrodite worms expressing IFY-1-GFP, GFP-CYB-1 or GFP alone and subjected to an immunoprecipitation (IP) assay. Immunoprecipitants with anti-GFP rabbit polyclonal antibody or control rabbit IgG were separated by SDS-PAGE and transferred to a PVDF membrane, which was then divided at the position of the 102 kDa marker protein. (**A**) The top portion of the membrane (proteins larger than 102 kDa) was western blotted (WB) with anti-ETC-1 antibody. (**B**) The bottom portion (proteins smaller than 102 kDa) was blotted with anti-GFP mouse monoclonal antibody. The top and bottom panels of B show X-ray film exposures for 30 seconds and 5 minutes, respectively.

1, embryos were arrested in the 1-cell stage. Chromosomes in arrested embryos were eventually decondensed, and a nuclear membrane formed around each mass of scattered DNA without cell division. Thus, aged embryos became 1-cell embryos with multiple small nuclei (Fig. 4A). The GFP-CYB-1 fluorescence signal was diminished in these arrested *ify-1*(RNAi) embryos. We optimized the condition for co-depletion of IFY-1 and ETC-1 by the feeding method, and confirmed that the efficiency of IFY-1 knockdown in the *ify-1*(RNAi); *etc-1*(RNAi) gonad was comparable to that in *ify-1*(RNAi) alone using IFY-1-GFP-expressing worms (supplementary material Fig. S8). *ify-1*(RNAi); *etc-1*(RNAi) embryos expressing GFP-CYB-1 were also arrested at the 1-cell stage.

If accumulation of GFP-CYB-1 in *etc-1*(RNAi) embryos is a consequence of IFY-1 accumulation, which titrates APC/C, co-depletion of IFY-1 should prevent CYB-1 accumulation. However, accumulation of GFP-CYB-1 was comparable in *ify-1*(RNAi); *etc-1*(RNAi) and *etc-1*(RNAi) embryos (Fig. 4A,B). Thus, ETC-1 depletion caused accumulation of GFP-CYB-1 regardless of the cellular IFY-1 level. These results suggest that ETC-1 regulates CYB-1 stability in postmeiotic embryos independently of IFY-1. Thus, IFY-1 might not help to regulate CYB-1 levels in postmeiotic embryos. Instead, we found that IFY-1 knockdown affected CYB-1 levels in embryos at the +1 position (immediately after fertilization). In contrast to wild-type embryos at the +1 position, in which the intensity of GFP-CYB-1 remained high (103% of the intensity of the oocyte at the –1 position), *ify-1*(RNAi) embryos at the +1 position retained only 53% of the GFP-CYB-1 intensity of the oocyte at the –1 position (Fig. 4B). This suggests that depletion of IFY-1 accelerated CYB-1 degradation during meiosis in embryos.

As this effect only occurred in embryos with normal levels of ETC-1 [wild type versus *ify-1*(RNAi)], IFY-1 might compete with CYB-1 during meiotic division for ETC-1-dependent degradation.

We next tested whether ETC-1 physically interacts with CYB-1 as well as with IFY-1 *in vivo*. We generated anti-ETC-1 rabbit polyclonal antibody, which specifically reacts with endogenous ETC-1 in whole-worm lysate (supplementary material Fig. S9), to analyze whether ETC-1 co-immunoprecipitates with CYB-1 (Fig. 5). When GFP-CYB-1 was ectopically expressed in worms and immunoprecipitated with anti-GFP antibody or rabbit IgG from whole-worm lysate, endogenous ETC-1 was specifically detected in the GFP immunoprecipitate but not in the IgG immunoprecipitate. Endogenous ETC-1 also co-immunoprecipitated with IFY-1-GFP but not GFP alone, confirming that our immunoprecipitation assay identified specific interaction of ETC-1 with IFY-1 and CYB-1. Association of ETC-1 with IFY-1 and CYB-1 was also demonstrated in an *in vitro* GST pull-down assay. ^{35}S-labeled His6-IFY-1 or CYB-1-His6 expressed in the rabbit reticulocyte system was co-purified with GST-ETC-1 bound to GST-Sepharose beads (supplementary material Fig. S10). Taken together, these results support the proposal that ETC-1 directly associates with CYB-1, as well as with IFY-1, to regulate their dynamics during and after meiosis.

ETC-1 ubiquitylates IFY-1 and CYB-1 *in vitro*

ETC-1 has the E3 ligase motif containing a HECT domain. Given that ETC-1 binds IFY-1, we hypothesized that ETC-1 ubiquitylates IFY-1 for ubiquitin-mediated proteolysis. We established an *in vitro* system to assess the ubiquitin ligase activity of ETC-1 using bacterially expressed and purified recombinant proteins. *C. elegans* has 22 proteins with homology to E2 ubiquitin-conjugating enzymes (Kipreos, 2005). Previously reported mutant phenotypes and RNAi phenotypes suggest that the E2 enzymes UBC-2 and UBC-18 can function during germ cell development. UBC-2 functions with the ring domain E3 ligase APC-11 (an APC/C constituent) during meiosis (Frazier et al., 2004). UBC-18 functions with the ARI-1 E3 ligase to regulate pharyngeal development (Qiu and Fay, 2006) and with the WWP-1 E3 ligase to regulate diet restriction-induced longevity (Carrano et al., 2009). In addition, RNAi knockdown of UBC-18 causes a reduction of brood size, suggesting its function in germ cell development (Fay et al., 2003).

We first tested UBC-2 and UBC-18 for *in vitro* ubiquitin ligase activity of ETC-1. When an E3 ligase protein is incubated with its functional E2 partner and HA-ubiquitin, ligase activity promotes the conjugation of HA-ubiquitin to E3 ligases or E2 enzymes as a step prior to the ubiquitylation of substrate proteins. Therefore, E3 ligase activity can be assessed in the absence of substrate proteins by the formation of high molecular weight HA-ubiquitin conjugates with E3 and E2, which can be detected by western blotting with anti-HA antibody. ETC-1 exhibited robust ubiquitin ligase activity with UBC-18 but not UBC-2 (supplementary material Fig. S11).

Next, we tested whether IFY-1 and CYB-1 were *in vitro* substrates for ETC-1. When bacterially expressed and purified His6-IFY-1 and CYB-1-His6 were added to the system, modified forms of proteins were detected as multiple bands in the reaction containing both ETC-1 and UBC-18 concomitantly with robust E3 ligase activity (Fig. 6). These protein modifications were not detected in the reaction containing GST-WWP-1, which also exhibited a robust E3 ligase activity with UBC-18. When His6-GFP was added as a negative

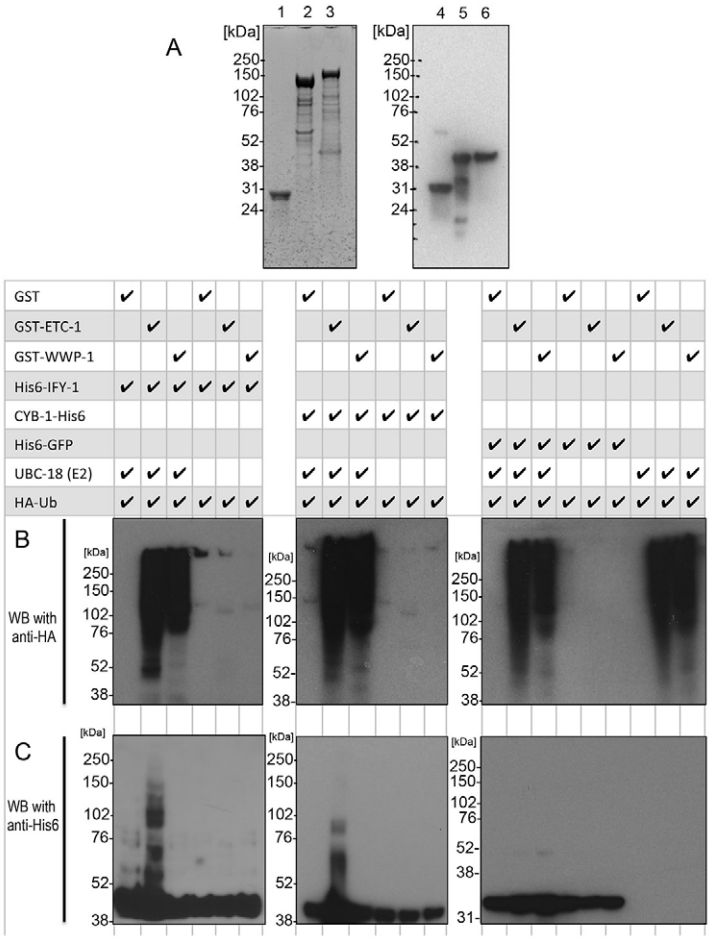

Fig. 6. *In vitro* ubiquitylation assays with purified recombinant proteins. (**A**) GST-fused proteins (lanes 1-3) and His6-tagged proteins (lanes 4-6) used for ubiquitylation assays are visualized by Simply Blue staining and western blotting with anti-penta His antibody, respectively. 1, GST; 2, GST-WWP-1; 3, GST-ETC-1; 4, His6-EGFP; 5, His6-IFY-1; 6, CYB-1-His6. (**B**,**C**) Ubiquitylation reactions containing the indicated proteins were divided in two, and each half was separated by SDS-PAGE and transferred to a PVDF membrane. One membrane was probed with anti-HA antibody to identify HA-ubiquitin-conjugated proteins (B) and the other was probed with anti-penta His antibody to identify modified His6-tagged proteins (C). In the HA blot, ubiquitylation activity was assessed by the formation of high molecular weight ubiquitin conjugates that form because of conjugation of ubiquitin to itself, E3 ligases or UBC-18, regardless of the presence or absence of substrate proteins. Robust ubiquitin ligase activity was detected in reactions containing GST-ETC-1 and UBC-18 or containing GST-WWP-1 and UBC-18. However, modified forms of His6-IFY-1 and CYB-1-His6 were detected only in reactions containing GST-ETC-1 and UBC-18. No modified form of His6-EGFP was detected in the reaction containing GST-ETC-1 and UBC-18.

control substrate, there was no modification even in the presence of active ETC-1 and UBC-18, suggesting that IFY-1 and CYB-1 were specifically ubiquitylated by ETC-1 in a UBC-18-dependent manner. Consistent with this result, RNAi knockdown of UBC-18 increased the stability of IFY-1 in embryos in post-meiosis I (supplementary material Fig. S12). Since UBC-18 functions in pharyngeal development in parallel with LIN-35/Rb, UBC-18 depletion in a *lin-35* mutant causes a synthetic lethal phenotype (Fay et al., 2003). By contrast, RNAi knockdown of ETC-1 in the *lin-35* mutant in our study did not affect the viability of mutant worms (supplementary material Fig. S13), suggesting that UBC-18 functions with ETC-1 specifically in germ cells in a manner that is distinct from its other functions.

ETC-1 functions redundantly with APC/C in meiosis I

ETC-1 knockdown under our experimental conditions caused elevated levels of cytoplasmic IFY-1 and CYB-1 in post-meiosis I embryos and extended the duration of meiosis II. Nevertheless, these changes did not affect brood size or the viability of progeny in a wild-type genetic background. However, ETC-1 knockdown substantially reduced the viability of progeny in combination with reduction of APC/C activity (Fig. 7A). *mat-1*(*ax161ts*) is a temperature-sensitive allele of the APC/C component *apc-3* (also known as *mat-1*) (Shakes et al., 2003). At the restrictive temperature (25°C), *mat-1*(*ax161ts*) homozygotes exhibit a strict metaphase-to-anaphase transition (*mat*)-defective phenotype. At the permissive temperature (16°C), although their brood size is smaller than of the wild type, most *mat-1*(*ax161ts*) embryos complete meiosis and develop in a manner indistinguishable from the wild type (Golden et al., 2000; Wallenfang and Seydoux, 2000). ETC-1 knockdown in *mat-1*(*ax161ts*) worms caused an embryonic lethal phenotype at 16°C.

To determine the cause of the embryonic lethality of *mat-1*(*ax161ts*) *etc-1*(RNAi) at the permissive temperature, we generated a strain expressing mCherry-histone H2B that was homozygous for *mat-1*(*ax161ts*) and analyzed chromosome morphology in developing germ cells and embryos. When depleted of ETC-1 at 16°C, *mat-1*(*ax161ts*) embryos were arrested before anaphase I, similar to embryos shifted to the restrictive temperature (Fig. 7B). Thus, the *mat-1*(*ax161ts*) *etc-1*(RNAi) phenotype at 16°C was comparable to that of *mat-1*(*ax161ts*) at 25°C.

An embryonic lethal phenotype also occurred with ETC-1 knockdown in combination with *fzy-1*(*h1983*), a hypomorphic allele of *fzy-1* that suppresses lethality caused by loss of spindle assembly checkpoint activity (Kitagawa et al., 2002). Mutant protein expressed from *h1983* cannot bind IFY-1. Furthermore, IFY-1 stability is increased in *fzy-1*(*h1983*) embryos (Tarailo et al., 2007). Thus, although ETC-1 activity is dispensable during meiosis I in the presence of an intact APC/C, it becomes essential for progression of meiosis I when APC/C activity is compromised, suggesting that ETC-1 and APC/C function redundantly to maintain the cytoplasmic level of IFY-1 and CYB-1 during meiosis I. Consistent with this, overexpression of CYB-1 also sensitized worms to ETC-1 knockdown (Fig. 7A).

In addition to the defect in metaphase-to-anaphase transition during meiosis I, we found premature NEBD in four out of 30 *mat-1*(*ax161ts*) *etc-1*(RNAi) gonad arms (Fig. 7B). NEBD marks the transition from meiotic prophase to metaphase, and is characteristic of this transition as it occurs occurring during oocyte maturation (McCarter et al., 1999). In the wild-type gonad, NEBD is restricted to the oocyte at the –1 position (the most proximal oocyte next to a spermatheca). Mature oocytes are fertilized within 6 minutes of NEBD. By contrast, in the *mat-1*(*ax161ts*) *etc-1*(RNAi) gonad,

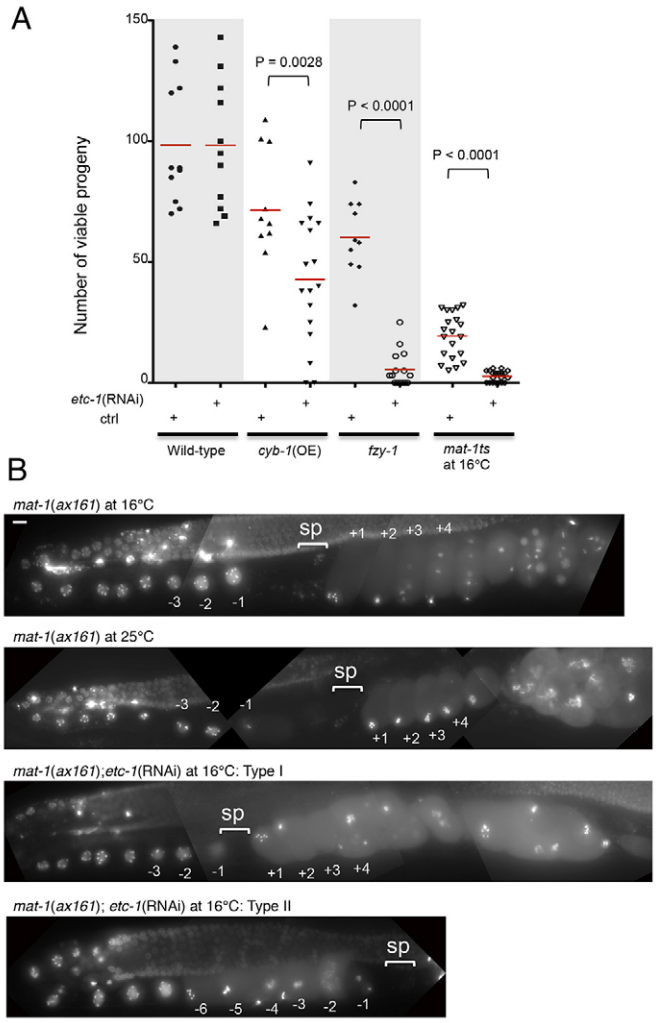

Fig. 7. *etc-1*(RNAi) causes synthetic lethality with reduced APC activity. (**A**) Worms of the indicated genotypes were treated, or otherwise, with *etc-1*(RNAi) and the number of viable progeny was scored. Wild type, N2; *cyb-1*(OE), RQ414 (expressing GFP-CYB-1); *fzy-1*, RQ47 [*fzy-1*(*h1983*) II]; *mat-1ts* at 16°C, DS77M [*mat-1*(*ax161*) I] at permissive temperature. Each symbol represents the number of viable progeny segregated from a single parent within 72 hours of starting RNAi treatment. *etc-1*(RNAi) substantially reduced the viability of progeny in RQ414 and RQ47 at 22°C and in DS77M at 16°C. *P*-values compared with untreated controls are shown. Red bars indicate mean values. (**B**) Embryos carrying the *mat-1*(*ax161ts*) mutation and expressing mCherry-histone H2B were treated with *etc-1*(RNAi) or shifted to a restrictive temperature (25°C), and the chromosome morphology of germ cells in the proximal region of the gonad arm was analyzed by fluorescence microscopy. The spermatheca (sp) and embryo positions relative to ovulation are indicated. Two types of germ cell developmental defect were observed in the *mat-1*(*ax161*) *etc-1*(RNAi) gonad: (type I) a metaphase-to-anaphase I transition defect similar to the phenotype of the *mat-1*(*ax161*) mutant shifted to 25°C; (type II) premature NEBD and failure to proceed with meiosis II. The timing of NEBD was determined by monitoring the diffusion of free mCherry-histone H2B out of the nucleus (free mCherry-histone H2B accumulates in the nucleus while the nuclear envelope is intact). Scale bar: 10 μm.

NEBD occurred in premature oocytes located in the middle of the proximal region of the gonad arm. After NEBD, oocytes proceeded with meiosis I division, producing a polar body, but did not enter meiosis II, and the chromosomes decondensed before fertilization.

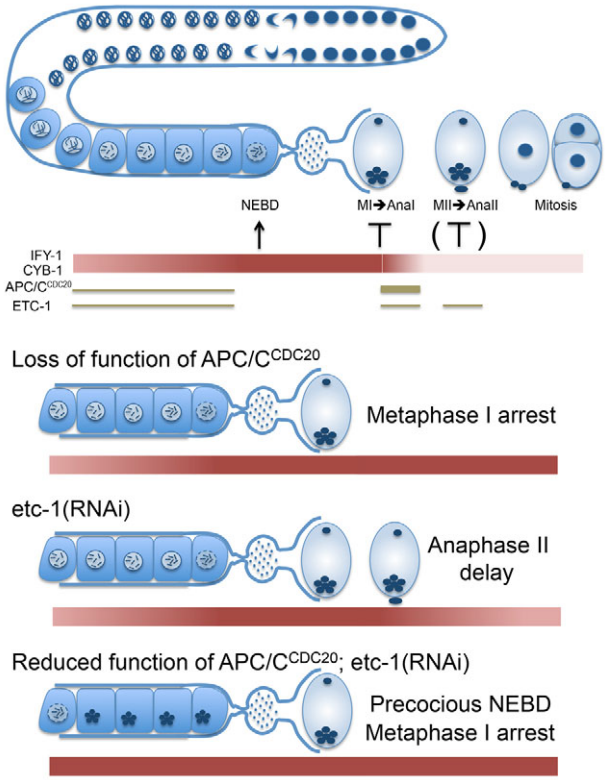

Fig. 8. APC/C and ETC-1 cooperatively regulate the dynamics of IFY-1 and CYB-1 during meiotic progression. APC/C and ETC-1 control the dynamics of IFY-1 and CYB-1 protein during meiosis for timely anaphase onset and NEBD. Depletion of ETC-1 causes delay in anaphase II. ETC-1 also functions cooperatively with APC/C during prophase I and onset of anaphase I.

This premature NEBD phenotype was not observed in gonads when *mat-1*(*ax161ts*) animals were shifted to 25°C or when ETC-1 was knocked down in a wild-type background. These results suggest that ETC-1 and APC/C function cooperatively to maintain oocyte nuclei in diakinesis (the final stage of prophase I) until oocytes are positioned at the most proximal region of the gonad arm.

DISCUSSION

The physiological function of ETC-1 during germ cell development

We have identified that the HECT domain-containing E3 ligase ETC-1 regulates the cytoplasmic level of IFY-1 and CYB-1 during meiotic progression, probably by targeting these proteins for ubiquitin-mediated proteolysis. As both IFY-1 and CYB-1 are crucial mitotic substrates of APC/C, it is possible that ETC-1 controls their stability by regulating APC/C activity. However, ETC-1 physically associates with IFY-1 and CYB-1 and ubiquitylates them *in vitro*. Therefore, it is more likely that ETC-1 functions independently of APC/C. Unlike loss of APC/C activity, which causes strict arrest at metaphase I, depletion of ETC-1 in a wild-type background substantially increased the stability of IFY-1 and CYB-1 during meiosis II and caused a delay in anaphase II; no other changes in meiotic progression were evident. However, ETC-1 knockdown under reduced APC/C activity revealed that ETC-1 functions in meiosis I redundantly with APC/C (Fig. 8). In mammals, APC/C activity and inactivation of CDK1 by separase are required to reduce cyclin B1 levels sufficiently to allow meiosis I to complete (Gorr et al., 2006). Therefore, our finding that APC/C is not the sole factor driving the completion of meiosis I in *C. elegans* supports a proposal that there are similar regulatory mechanisms of meiotic progression in worms and mammals. Reduction of activity of ETC-1 and APC/C also caused the premature NEBD phenotype with low-penetrance during prophase I. In mammalian oocytes, APC/C activity is required to maintain low cyclin B1 levels during prophase I arrest (Reis et al., 2007; Holt et al., 2011). CYB-1-dependent phosphorylation of the nuclear pore component NPP-12 (Gp210) is required for timely NEBD during mitosis (Galy et al., 2008). Consistent with this, CYB-1 depletion causes a delay in NEBD (Galy et al., 2008; van der Voet et al., 2009). Given that both ETC-1 and APC/C target CYB-1 for ubiquitin-mediated proteolysis, premature NEBD in *mat-1*(*ax161ts*) *etc-1*(RNAi) might be due to dysregulation of CYB-1.

Recently, Green et al. reported (as part of an RNAi-based functional analysis of 554 essential genes, using gonad morphology as a substrate for high-content phenotypic profiling) that ETC-1 knockdown causes several morphological defects in gonad architecture, including delayed oocyte budding (Green et al., 2011). We obtained the strain used by Green et al. that expresses fluorescent markers to visualize the plasma membrane and chromosomes and confirmed that RNAi-mediated depletion of ETC-1 using our feeding method caused the delayed oocyte budding phenotype (supplementary material Fig. S14). Interestingly, in their assay Green et al. (Green et al., 2011) also observed a delayed oocyte budding phenotype upon knockdown of APC/C components and separase, suggesting that common targets of APC/C and ETC-1, such as IFY-1 and CYB-1, are involved in regulating the timing of oocyte budding. Further studies are needed to elucidate the ETC-1 substrates responsible for the abnormalities observed in the *etc-1*(RNAi) gonad.

Predicted function of ETC-1 in cytoplasmic protein homeostasis

It has been reported that ETC-1 knockdown by RNAi causes sterility (Maeda et al., 2001). However, under our experimental conditions ETC-1 knockdown did not have a severe effect on fertility in a wild-type genetic background. We also tested RNAi by the soaking method and the microinjection method, but found no increase in the severity of phenotypes (our unpublished observations). Furthermore, we recently found that a worm strain homozygous for the *etc-1* deletion allele *tm5615* (kindly provided by Dr S. Mitani) is viable and fertile (our unpublished observations). Since *tm5615* deletes only exons 3 and 4 of *etc-1*, a truncated yet functional protein might be expressed in *tm5615* homozygotes. Although our phenotypic analysis of *etc-1*(RNAi) or *etc-1*(*tm5615*) homozygotes did not identify significant developmental defects, when GFP-fused ETC-1 was exogenously expressed by the *pie-1* promoter, a substantial amount of GFP-ETC-1 accumulated in the epidermal tissues of L1 larvae (supplementary material Fig. S6B), suggesting a role for ETC-1 in postembryonic development. This function of ETC-1 might be evident only when other proteins functioning in parallel are simultaneously depleted.

ETC-1 is a HECT domain-containing E3 ligase and has amino acid sequence similarity to budding yeast Hul5. It was recently shown that Hul5 plays an important role in ubiquitylating cytosolic misfolded proteins to maintain protein homeostasis in response to heat shock (Fang et al., 2011). In *C. elegans*, ubiquitin-mediated proteolysis of misfolded or aggregated proteins is also proposed as a primary mechanism to maintain protein quality. Consistent with this, it has been shown that inhibition of the proteasome and RNAi knockdown of CUL-1 and CUL-2 increase sensitivity to the

expression of toxic polyglutamine repeat proteins (Mehta et al., 2009). However, they also showed that ETC-1 knockdown caused the opposite effect: ETC-1 knockdown worms were more resistant to the accumulation of toxic aggregated proteins (Mehta et al., 2009). This suggests that ETC-1 knockdown stabilizes stress response proteins to keep the stress response pathway active. Given that FZY-1 knockdown did not affect sensitivity to the accumulation of aggregated proteins, the target of ETC-1 responsible for the phenotype is unlikely to be IFY-1 or CYB-1.

Taken together, our results support the proposal that ETC-1 is required for the immediate removal of proteins that are transiently accumulated in the cytoplasm, so that the cytosolic protein concentration is brought back to a level that enables cells to quickly restore their normal status.

Acknowledgements
We thank the *Caenorhabditis* Genetics Center for strains; Andrea Carrano, Andrew Dillin, Robert Barstead, Shohei Mitani, Ann M. Rose, Lynn Boyd and Josef Loidl for generous gifts of reagents; and Edward Kipreos and Andy Golden for critical reading of the manuscript.

Funding
This work was supported by the Ohio Cancer Research Associates Seed Grant to R.K.

Competing interests statement
The authors declare no competing financial interests.

Supplementary material
Supplementary material available online at
http://dev.biologists.org/lookup/suppl/doi:10.1242/dev.090688/-/DC1

References

Bao, Z., Zhao, Z., Boyle, T. J., Murray, J. I. and Waterston, R. H. (2008). Control of cell cycle timing during C. elegans embryogenesis. *Dev. Biol.* **318**, 65-72.
Carrano, A. C., Liu, Z., Dillin, A. and Hunter, T. (2009). A conserved ubiquitination pathway determines longevity in response to diet restriction. *Nature* **460**, 396-399.
Cheeseman, I. M., Niessen, S., Anderson, S., Hyndman, F., Yates, J. R., 3rd, Oegema, K. and Desai, A. (2004). A conserved protein network controls assembly of the outer kinetochore and its ability to sustain tension. *Genes Dev.* **18**, 2255-2268.
Davis, E. S., Wille, L., Chestnut, B. A., Sadler, P. L., Shakes, D. C. and Golden, A. (2002). Multiple subunits of the Caenorhabditis elegans anaphase-promoting complex are required for chromosome segregation during meiosis I. *Genetics* **160**, 805-813.
Deyter, G. M., Furuta, T., Kurasawa, Y. and Schumacher, J. M. (2010). Caenorhabditis elegans cyclin B3 is required for multiple mitotic processes including alleviation of a spindle checkpoint-dependent block in anaphase chromosome segregation. *PLoS Genet.* **6**, e1001218.
Fang, N. N., Ng, A. H., Measday, V. and Mayor, T. (2011). Hul5 HECT ubiquitin ligase plays a major role in the ubiquitylation and turnover of cytosolic misfolded proteins. *Nat. Cell Biol.* **13**, 1344-1352.
Fay, D. S., Large, E., Han, M. and Darland, M. (2003). lin-35/Rb and ubc-18, an E2 ubiquitin-conjugating enzyme, function redundantly to control pharyngeal morphogenesis in C. elegans. *Development* **130**, 3319-3330.
Frazier, T., Shakes, D., Hota, U. and Boyd, L. (2004). Caenorhabditis elegans UBC-2 functions with the anaphase-promoting complex but also has other activities. *J. Cell Sci.* **117**, 5427-5435.
Furuta, T., Tuck, S., Kirchner, J., Koch, B., Auty, R., Kitagawa, R., Rose, A. M. and Greenstein, D. (2000). EMB-30: an APC4 homologue required for metaphase-to-anaphase transitions during meiosis and mitosis in Caenorhabditis elegans. *Mol. Biol. Cell* **11**, 1401-1419.
Galy, V., Antonin, W., Jaedicke, A., Sachse, M., Santarella, R., Haselmann, U. and Mattaj, I. (2008). A role for gp210 in mitotic nuclear-envelope breakdown. *J. Cell Sci.* **121**, 317-328.
Golden, A., Sadler, P. L., Wallenfang, M. R., Schumacher, J. M., Hamill, D. R., Bates, G., Bowerman, B., Seydoux, G. and Shakes, D. C. (2000). Metaphase to anaphase (mat) transition-defective mutants in Caenorhabditis elegans. *J. Cell Biol.* **151**, 1469-1482.
Gorr, I. H., Reis, A., Boos, D., Wühr, M., Madgwick, S., Jones, K. T. and Stemmann, O. (2006). Essential CDK1-inhibitory role for separase during meiosis I in vertebrate oocytes. *Nat. Cell Biol.* **8**, 1035-1037.
Green, R. A., Kao, H. L., Audhya, A., Arur, S., Mayers, J. R., Fridolfsson, H. N., Schulman, M., Schloissnig, S., Niessen, S., Laband, K. et al. (2011). A high-resolution C. elegans essential gene network based on phenotypic profiling of a complex tissue. *Cell* **145**, 470-482.
Holt, L. J., Krutchinsky, A. N. and Morgan, D. O. (2008). Positive feedback sharpens the anaphase switch. *Nature* **454**, 353-357.
Holt, J. E., Tran, S. M., Stewart, J. L., Minahan, K., García-Higuera, I., Moreno, S. and Jones, K. T. (2011). The APC/C activator FZR1 coordinates the timing of meiotic resumption during prophase I arrest in mammalian oocytes. *Development* **138**, 905-913.
Jallepalli, P. V., Waizenegger, I. C., Bunz, F., Langer, S., Speicher, M. R., Peters, J. M., Kinzler, K. W., Vogelstein, B. and Lengauer, C. (2001). Securin is required for chromosomal stability in human cells. *Cell* **105**, 445-457.
Jensen, S., Segal, M., Clarke, D. J. and Reed, S. I. (2001). A novel role of the budding yeast separin Esp1 in anaphase spindle elongation: evidence that proper spindle association of Esp1 is regulated by Pds1. *J. Cell Biol.* **152**, 27-40.
Kamath, R. S. and Ahringer, J. (2003). Genome-wide RNAi screening in Caenorhabditis elegans. *Methods* **30**, 313-321.
Kipreos, E. T. (2005). Ubiquitin-mediated pathways in C. elegans. *WormBook* **2005**, 1-24.
Kitagawa, R., Law, E., Tang, L. and Rose, A. M. (2002). The Cdc20 homolog, FZY-1, and its interacting protein, IFY-1, are required for proper chromosome segregation in Caenorhabditis elegans. *Curr. Biol.* **12**, 2118-2123.
Lee, J., Iwai, T., Yokota, T. and Yamashita, M. (2003). Temporally and spatially selective loss of Rec8 protein from meiotic chromosomes during mammalian meiosis. *J. Cell Sci.* **116**, 2781-2790.
Liu, J., Vasudevan, S. and Kipreos, E. T. (2004). CUL-2 and ZYG-11 promote meiotic anaphase II and the proper placement of the anterior-posterior axis in C. elegans. *Development* **131**, 3513-3525.
Maeda, I., Kohara, Y., Yamamoto, M. and Sugimoto, A. (2001). Large-scale analysis of gene function in Caenorhabditis elegans by high-throughput RNAi. *Curr. Biol.* **11**, 171-176.
Marangos, P. and Carroll, J. (2008). Securin regulates entry into M-phase by modulating the stability of cyclin B. *Nat. Cell Biol.* **10**, 445-451.
McCarter, J., Bartlett, B., Dang, T. and Schedl, T. (1999). On the control of oocyte meiotic maturation and ovulation in Caenorhabditis elegans. *Dev. Biol.* **205**, 111-128.
McGuinness, B. E., Anger, M., Kouznetsova, A., Gil-Bernabé, A. M., Helmhart, W., Kudo, N. R., Wuensche, A., Taylor, S., Hoog, C., Novak, B. et al. (2009). Regulation of APC/C activity in oocytes by a Bub1-dependent spindle assembly checkpoint. *Curr. Biol.* **19**, 369-380.
Meacci, G., Ries, J., Fischer-Friedrich, E., Kahya, N., Schwille, P. and Kruse, K. (2006). Mobility of Min-proteins in Escherichia coli measured by fluorescence correlation spectroscopy. *Phys. Biol.* **3**, 255-263.
Mehta, R., Steinkraus, K. A., Sutphin, G. L., Ramos, F. J., Shamieh, L. S., Huh, A., Davis, C., Chandler-Brown, D. and Kaeberlein, M. (2009). Proteasomal regulation of the hypoxic response modulates aging in C. elegans. *Science* **324**, 1196-1198.
Musacchio, A. and Salmon, E. D. (2007). The spindle-assembly checkpoint in space and time. *Nat. Rev. Mol. Cell Biol.* **8**, 379-393.
Nabti, I., Reis, A., Levasseur, M., Stemmann, O. and Jones, K. T. (2008). Securin and not CDK1/cyclin B1 regulates sister chromatid disjunction during meiosis II in mouse eggs. *Dev. Biol.* **321**, 379-386.
Parisi, S., McKay, M. J., Molnar, M., Thompson, M. A., van der Spek, P. J., van Drunen-Schoenmaker, E., Kanaar, R., Lehmann, E., Hoeijmakers, J. H. and Kohli, J. (1999). Rec8p, a meiotic recombination and sister chromatid cohesion phosphoprotein of the Rad21p family conserved from fission yeast to humans. *Mol. Cell. Biol.* **19**, 3515-3528.
Pasierbek, P., Jantsch, M., Melcher, M., Schleiffer, A., Schweizer, D. and Loidl, J. (2001). A Caenorhabditis elegans cohesion protein with functions in meiotic chromosome pairing and disjunction. *Genes Dev.* **15**, 1349-1360.
Pesin, J. A. and Orr-Weaver, T. L. (2008). Regulation of APC/C activators in mitosis and meiosis. *Annu. Rev. Cell Dev. Biol.* **24**, 475-499.
Praitis, V., Casey, E., Collar, D. and Austin, J. (2001). Creation of low-copy integrated transgenic lines in Caenorhabditis elegans. *Genetics* **157**, 1217-1226.
Qiu, X. and Fay, D. S. (2006). ARI-1, an RBR family ubiquitin-ligase, functions with UBC-18 to regulate pharyngeal development in C. elegans. *Dev. Biol.* **291**, 239-252.
Queralt, E., Lehane, C., Novak, B. and Uhlmann, F. (2006). Downregulation of PP2A(Cdc55) phosphatase by separase initiates mitotic exit in budding yeast. *Cell* **125**, 719-732.
Reis, A., Madgwick, S., Chang, H. Y., Nabti, I., Levasseur, M. and Jones, K. T. (2007). Prometaphase APCcdh1 activity prevents non-disjunction in mammalian oocytes. *Nat. Cell Biol.* **9**, 1192-1198.
Shakes, D. C., Sadler, P. L., Schumacher, J. M., Abdolrasulnia, M. and Golden, A. (2003). Developmental defects observed in hypomorphic anaphase-promoting complex mutants are linked to cell cycle abnormalities. *Development* **130**, 1605-1620.
Shakes, D. C., Allen, A. K., Albert, K. M. and Golden, A. (2011). emb-1 encodes the APC16 subunit of the Caenorhabditis elegans anaphase-promoting complex. *Genetics* **189**, 549-560.

Siomos, M. F., Badrinath, A., Pasierbek, P., Livingstone, D., White, J., Glotzer, M. and Nasmyth, K. (2001). Separase is required for chromosome segregation during meiosis I in Caenorhabditis elegans. *Curr. Biol.* **11**, 1825-1835.
Sonneville, R. and Gönczy, P. (2004). Zyg-11 and cul-2 regulate progression through meiosis II and polarity establishment in C. elegans. *Development* **131**, 3527-3543.
Stegmeier, F., Visintin, R. and Amon, A. (2002). Separase, polo kinase, the kinetochore protein Slk19, and Spo12 function in a network that controls Cdc14 localization during early anaphase. *Cell* **108**, 207-220.
Tarailo, M., Kitagawa, R. and Rose, A. M. (2007). Suppressors of spindle checkpoint defect (such) mutants identify new mdf-1/MAD1 interactors in Caenorhabditis elegans. *Genetics* **175**, 1665-1679.
van der Voet, M., Lorson, M. A., Srinivasan, D. G., Bennett, K. L. and van den Heuvel, S. (2009). C. elegans mitotic cyclins have distinct as well as overlapping functions in chromosome segregation. *Cell Cycle* **8**, 4091-4102.
Vasudevan, S., Starostina, N. G. and Kipreos, E. T. (2007). The Caenorhabditis elegans cell-cycle regulator ZYG-11 defines a conserved family of CUL-2 complex components. *EMBO Rep.* **8**, 279-286.
Wallenfang, M. R. and Seydoux, G. (2000). Polarization of the anterior-posterior axis of C. elegans is a microtubule-directed process. *Nature* **408**, 89-92.
Watanabe, S., Yamamoto, T. G. and Kitagawa, R. (2008). Spindle assembly checkpoint gene mdf-1 regulates germ cell proliferation in response to nutrition signals in C. elegans. *EMBO J.* **27**, 1085-1096.
Xu, H., Beasley, M. D., Warren, W. D., van der Horst, G. T. and McKay, M. J. (2005). Absence of mouse REC8 cohesin promotes synapsis of sister chromatids in meiosis. *Dev. Cell* **8**, 949-961.
Yamamoto, A., Guacci, V. and Koshland, D. (1996). Pds1p, an inhibitor of anaphase in budding yeast, plays a critical role in the APC and checkpoint pathway(s). *J. Cell Biol.* **133**, 99-110.